ELSEVIER

Materials Science and Engineering A xxx (2004) xxx–xxx

MATERIALS SCIENCE & ENGINEERING A

www.elsevier.com/locate/msea

The role of ab initio electronic structure calculations in studies of the strength of materials

M. Šob [a,*], M. Friák [a,b], D. Legut [a,c], J. Fiala [c], V. Vitek [d]

[a] *Institute of Physics of Materials, Academy of Sciences of the Czech Republic, Žižkova 22, Brno CZ-616 62, Czech Republic*
[b] *Institute of Condensed Matter Physics, Faculty of Science, Masaryk University, Kotlářská 2, Brno CZ-611 37, Czech Republic*
[c] *Institute of Chemistry of Materials, Faculty of Chemistry, Brno University of Technology, Purkyňova 118, Brno CZ-612 00, Czech Republic*
[d] *Department of Materials Science and Engineering, University of Pennsylvania, 3231 Walnut St., Philadelphia, PA 19104-6272, USA*

Received 25 August 2003; received in revised form 18 October 2003

Abstract

In this paper we give an account of applications of quantum-mechanical (first-principles) electronic structure calculations to the problem of theoretical tensile strength in metals and intermetallics. First, we review previous as well as ongoing research on this subject. We then describe briefly the electronic structure calculational methods and simulation of the tensile test. This approach is then illustrated by calculations of theoretical tensile strength in iron and in the intermetallic compound Ni_3Al. The anisotropy of calculated tensile strength is explained in terms of higher-symmetry structures encountered along the deformation paths studied. The table summarizing values of theoretical tensile strengths calculated up to now is presented and the role of ab initio electronic structure calculations in contemporary studies of the strength of material is discussed.

Keywords: Ab initio electronic structure calculations; Theoretical tensile strength; Non-linear elasticity; Magnetism; Metals; Intermetallic compounds

1. Introduction

The electronic structure (ES) of materials, which in the general sense determines all their physical properties, can be determined accurately by ab initio (first-principles) ES calculations, i.e. from fundamental quantum theory. Here the atomic numbers of constituent atoms and, usually, some structural information are employed as the only input data. Such calculations are routinely performed within the framework of the density functional theory in which the complicated many-body interaction of all electrons is replaced by an equivalent but simpler problem of a single electron moving in an effective potential [1–3].[1] For a given material, the calculated total energies can be used to obtain equilibrium lattice parameters, elastic moduli, relative stabilities of competing crystal structures, energies associated with point and planar defects, etc. In addition, we also obtain information about electronic densities of states and charge densities that enables us to attain deeper insights and learn which aspects of the problem are important. The calculations are usually performed at zero temperature (0 K), but the results obtained often constitute the basis for understanding finite-temperature properties. Recently, determination of the theoretical strength of materials became possible using ab initio ES calculations.

In most engineering applications, the strength of materials is controlled by nucleation and motion of dislocations or microcracks. If such defects were not present, the material loaded in tension would only fail if the theoretical, or ideal tensile strength were reached. The stress at which this is achieved is comparable with the Young modulus of the material and it is an upper limit of stresses attainable prior to failure. Until recently, loads of this magnitude were approached in studies of the mechanical behaviour of whiskers of very pure metals and semiconductors [4–8]. However, the ideal strength appears to control both the onset of fracture and dislocation nucleation in defect-free thin films and, in

* Corresponding author. Tel.: +420 532 290 455; fax: +420 541 212 301.
E-mail addresses: mojmir@ipm.cz (M. Šob), mafri@ipm.cz (M. Friák), legut@ipm.cz (D. Legut), vitek@sol1.lrsm.upenn.edu (V. Vitek).

[1] In 1998, Walter Kohn and John Pople were awarded the Nobel Prize in Chemistry for developing and applying the density functional theory.

0921-5093/$ – see front matter © 2004 Elsevier B.V. All rights reserved.
doi:10.1016/j.msea.2003.10.376

particular, in nanostructured materials that are currently being developed. This has been confirmed most eloquently by nanoindentation experiments (see e.g. [9–14]) which suggest that the onset of yielding at the nanoscale is controlled by homogeneous nucleation of dislocations in the small volume under the nanoindenter where the stresses approach the theoretical strength. This volume is practically always dislocation-free, since in well-annealed samples the average dislocation spacing is about 1 μm, while the contact area, as well as the depth in which large stresses are attained, are of the order of 100 nm.

Theoretically, the ideal strength was studied in the past using semiempirical approaches when describing atomic interactions (for a review see e.g. [15] and the references therein; ideal shear strengths calculated for all basic cubic structures may be found in [16]). Within such schemes parameters characterizing interatomic forces are fitted to equilibrium properties of the material studied. However, their transferability to the state when this material is loaded close to its theoretical strength is not warranted. In contrast, ab initio ES calculations can be performed reliably for variously strained structures and are thus capable to determine the ideal strength of materials without the resort to doubtful extrapolations. Nevertheless, most of the ES calculations were directed towards finding the equilibrium state of a given material that corresponds to the minimum of the total energy or towards analysis of relatively small deviations from that state. On the other hand, theoretical strength is related to the maximum force that may be applied to the material before an instability occurs. It is usually connected with an inflexion point on the dependence of the total energy on deformation parameters.

The first paper dealing with the ideal tensile strength from the first-principles was probably that of Esposito et al. [17] who studied tensile deformation in Cu. However, these authors did not perform relaxations of dimensions of the loaded crystal in the directions perpendicular to the loading axis. Ideal shear strength was calculated in [18] (V, Cr, Nb, Mo, W, Al, Cu, Ir), [19] (Mo) and [20] (Ta), again without any relaxation. Other ab initio calculations of properties of the systems far from equilibrium have also been made, such as exploration of the structural stability, but the results were not employed to evaluate the strength [21–25].

Probably the first ab initio simulation of a tensile test, including the relaxation in perpendicular directions to the loading axis, was performed by Price et al. [26] for uniaxial loading of TiC along the [0 0 1] axis. Later, our group at the Institute of Physics of Materials in Brno in collaboration with the group at the University of Pennsylvania, Philadelphia, initiated systematic ab initio studies of theoretical strength and stability in metals and intermetallic compounds under extreme loading conditions. In [27], we obtained the theoretical tensile strengths for [0 0 1] and [1 1 1] loading axes in tungsten. The results compared very well with experiments performed on tungsten whiskers by Mikhailovskii et al. [28]. Further, we calculated ideal tensile strength in NiAl [29,30] and Cu [30]. These results established a basis for further calculations of ideal tensile strength. Li and Wang [31] computed the ideal tensile strength in Al. Further, Kitagawa and Ogata [32,33] studied the tensile strength of Al and AlN, but did not include Poisson contraction. The group of Cohen and Morris at the University of California at Berkeley calculated ideal shear strength in Al and Cu [34,35] as well as in W [36,37], performed a thorough theoretical analysis of the problem of strength and elastic stability [38] and, among others, verified our values of ideal tensile strength for tungsten [37]. Further calculations of the theoretical tensile strength were performed for β-SiC [39], diamond [40], Si and Ge [41], Mo and Nb [42], and for Si_3N_4 [43–45]. Ideal shear strength was recently calculated for TiC, TiN and HfC [46], Mo and Nb [42], Si [47] and newly for Al and Cu [48]. Some calculations have been done for nanowires (amorphous Si [49], MoSe nanowires [50]), grain boundaries [51–54], and interfaces [55,56].

From 1997, ab initio calculations of theoretical strength under hydrostatic tension (i.e., negative hydrostatic pressure) also appear [57–63]. As the symmetry of the structure does not change during this deformation, simpler ab initio approaches may be applied.

Recently, we have simulated a tensile test in prospective high-temperature materials, namely in transition metal disilicides $MoSi_2$ and WSi_2 with the $C11_b$ structure. These studies included calculation of the tensile strength for [0 0 1] loading and analysis of bonds and their changes during the test [64–66]. Theoretical tensile strength of iron in the loading direction [0 0 1] was determined in [67–72]; in [69,70], we compared the results obtained in [67,68] and calculated the tensile strength of iron for uniaxial loading in the [1 1 1] direction. As discussed in [69,71] and also in Section 4.1.2 of the present review, no magnetic instabilities occur prior to reaching the inflexion point in the energy versus elongation curve for uniaxial loading along the [0 0 1] and [1 1 1] directions as well as for the hydrostatic loading and, therefore, the calculated values of theoretical strength of iron are not influenced by magnetic effects.

Most ab initio calculations of theoretical strength up to now analyzed just the position of the inflexion point in the dependence of the total energy on the elongation which yields the maximum of the tensile stress during loading. If any other instability (violation of some stability condition, soft phonon modes, magnetic spin arrangement etc. [14,31,38,42,69,71,73–77]) does not occur prior to reaching this inflexion point, the maximum of the tensile stress also corresponds to the theoretical tensile strength. In principle, analysis of the phonon spectrum of a strained crystal at each point of the deformation path should be necessary and sufficient to ascertain the stability of the investigated material. Such an analysis based on ab initio calculations is, however, extremely demanding and has been made only in a very recent study of strength of Al by Clatterbuck et al. [78]. These authors performed ab initio calculations of the phonon spectra as a function of strain for uniaxial tension

along the [0 0 1], [1 1 0] and [1 1 1] directions as well as for relaxed ⟨1 1 2⟩{1 1 1} shear. They found that in all four cases, phonon instabilities determine the theoretical strength of Al. In some materials, another elastic stability criterion may be violated prior to reaching the inflexion point at the energy versus elongation curve. It was shown that this is the case of the [0 0 1] uniaxial loading in Al [31], in Nb [42] and, very recently, in Cu [77].

Tables summarizing ab initio values of theoretical tensile strengths for various materials are given in [69,79–82] and, most up-to date, in Table 1 in Section 5 of this paper. Ref. [80] includes also ab initio values of shear strengths and some semiempirical results. An extensive review of the semiempirical and ab initio calculated values of uniaxial and hydrostatic tensile strengths, as well as of shear strengths calculated up to 1999, can be found in [81]; an up-dated version of this database is in preparation [82].

The purpose of the present paper is to give an account of applications of the first-principles ES calculations to the problem of the theoretical tensile strength in metals and intermetallic compounds. First we briefly describe the way of simulating the tensile test (Section 2) and the ES calculational methods (Section 3). In the next part we present a study of iron and Ni_3Al as specific examples (Section 4). In Section 5, we summarize the values of the theoretical tensile strength calculated ab initio up to now, and in Section 6 we conclude by discussing the role of ab initio electronic structure calculations in contemporary studies of strength of materials.

2. Tensile test simulation

To simulate a uniaxial tensile test, we start by determining the structure and total energy of the material in the ground state. Then, in the second step, we apply an elongation along the loading axis by a fixed amount ε that is equivalent to application of a certain tensile stress σ. For each value of ε we minimize the total energy by relaxing the stresses σ_1 and σ_2 in the directions perpendicular to the loading axis. The stress σ is given by

$$\sigma = \frac{c}{V}\frac{\partial E}{\partial c} = \frac{1}{Ac_0}\frac{\partial E}{\partial \varepsilon} \tag{1}$$

where E is the total energy per repeat cell, V the volume of the repeat cell, c the dimension of the repeat cell in the direction of loading, A (equal to V/c ratio) the area of the basis of the repeat cell in the plane perpendicular to the loading axis, and c_0 the value of c in the undeformed state.

We are also interested in the tensile strength for hydrostatic tension. In this case, we start again with the material in its ground-state structure, and the dimensions of the crystal are gradually increased homogeneously in all directions. The hydrostatic stress σ is then calculated using the formula $\sigma = \mathrm{d}E/\mathrm{d}V$.

As stated at the end of the previous section, the inflexion point in the dependence of the total energy on the elongation yields the maximum of the tensile stress during loading and, in most ab initio studies up to now, this maximum stress was considered to be the theoretical tensile strength, σ_{th}. In some cases, however, other instabilities (soft phonons, magnetic transitions, violation of some other stability condition [14,31,38,42,69,71,73–78]) may occur prior to reaching the inflexion point; in this case, the stress corresponding to these instabilities determines the theoretical strength for a given mode of loading. Up to now, other elastic stability criteria were analyzed from the first-principles in W [27], Al [31], Mo and Nb [42], Fe [71] and Cu [77], magnetic instabilities were discussed in Fe [69,71] and the soft phonon modes were shown to play a key role in theoretical strength of Al [78].

3. Methods of electronic structure calculations

Most electronic structure calculations have been performed within the density functional theory [1–3]. Here the problem of many interacting electrons is transformed into study of the motion of a single electron in some effective potential. This is described by the Kohn–Sham equation, which is formally similar to the Schrödinger equation. In the case of periodic solids (crystals), we search the one-electron wave functions in the form of expansions using carefully chosen basis functions satisfying the Bloch condition.

Various methods used in the ES calculations may be distinguished according to the choice of the basis functions. The better we choose them (according to the character of the problem), the smaller number of them is needed for the description of one-electron wave functions. Commonly used bases are augmented (APW) and orthogonalized (OPW) plane waves, linear muffin-tin orbitals (LMTO), linear combination of atomic orbitals (LCAO), Gaussian (LCGO) and augmented Slater-type (LASTO) orbitals, augmented spherical waves (ASW), etc. The Korringa–Kohn–Rostoker (KKR) method proceeds by the use of the Green function of the Kohn–Sham equation and is also called Green function (GF) method. The pseudopotential approach, applied mostly to solids containing no d- or f-electrons, is also widely used. A detailed description of these methods may be found in many books and articles, e.g. in [83–86].

After choosing an appropriate basis, the Kohn–Sham equation is solved iteratively in order to attain selfconsistency, i.e., the electron density, determined from the effective one-electron potential, must generate the same effective potential (which is again a functional of the electron density). The quality and speed of the convergence of such calculations is related not only to the choice of a suitable basis, but also to the sophistication of the iterative process, where as a plausible input usually atomic-like potentials are employed and input and output potentials are appropriately mixed before starting a new iteration. Sometimes hundreds

of iterations are needed, e.g. in metallic materials with high peaks in the density of states alternating above and below the Fermi energy, or in most surface problems.

The atomic configurations corresponding to the deformed structures usually have a lower symmetry and, at the strength limit, they are very far from the lowest-energy equilibrium state. Therefore, to get reliable structural energy differences, we must use full-potential methods (i.e. without any shape approximation of the crystal potential and electronic charge density). At present, several codes are available, e.g. WIEN, VASP, FHI, FLEUR, FPLO, FPLMTO, ABINIT, SIESTA, etc. In this study, we have used the full-potential linearized augmented plane wave (FLAPW) code WIEN97 described in detail in [87]. The so-called exchange-correlation energy appearing in Kohn–Sham equations was evaluated within the generalized-gradient approximation (GGA) [88]. This is important especially for iron, since the local density approximation (LDA) does not render the ground state of iron correctly. The muffin-tin radius of iron atoms of 1.90 au was kept constant for all calculations. The number of k-points in the whole Brillouin zone was equal to 6000 and the product of the muffin-tin radius and the maximum reciprocal space vector, $R_{MT}k_{max}$, was set to 10. The maximum l value for the waves inside the atomic spheres, l_{max}, and the largest reciprocal vector in the Fourier expansion of the charge, G_{max}, was equal to 12 and 15, respectively. In the case of Ni_3Al, the muffin-tin radii of both Ni and Al atoms were equal to 2.0 au, number of k-points in the whole Brillouin zone was 4000, and the product $R_{MT}k_{max} = 8$. The values of l_{max} and G_{max} were 12 and 10, respectively.

4. Results and discussion

4.1. Iron

4.1.1. Total energies and magnetic states of tetragonally and trigonally deformed iron

First, we have calculated the total energy and magnetic moment of iron deformed along the tetragonal and trigonal paths at constant atomic volumes ranging from $V/V_{exp} = 0.84$ to 1.05, where V_{exp} is the experimental equilibrium atomic volume of the ferromagnetic bcc iron corresponding to the lattice constant $a_{bcc} = 2.862$ Å (5.408 au, 1 au = 1 bohr = 0.529177 Å). We included non-magnetic (NM), ferromagnetic (FM) and two antiferromagnetic states, namely the single-layer antiferromagnetic state (AFM1), in which the (0 0 1) or (1 1 1) planes have alternating magnetic moments (↑↓↑↓...), and the double-layer antiferromagnetic state (AFMD), where the pairs of (0 0 1) or (1 1 1) planes have alternating magnetic moments (↑↑↓↓...). The total energy of iron is plotted as a function of the volume and c/a ratio in Figs. 1 and 2. We show only those states the energies of which are the lowest for a given configuration. In Fig. 1, we can clearly see the "horseshoes" dividing the plane into the AFM1, AFMD

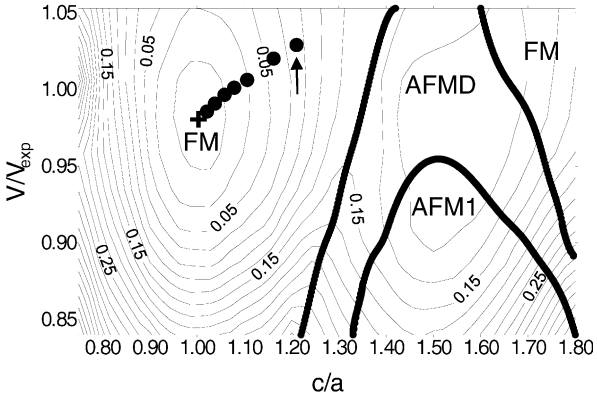

Fig. 1. Total energy (per atom) of iron as a function of the tetragonal c/a ratio and volume relative to the energy of the FM bcc ground state calculated within the GGA. Here the bcc structure corresponds to $c/a = 1$ and the fcc structure to $c/a=\sqrt{2}$ [21,23]. Only states with the minimum energy are shown. The contour interval is equal to 20 meV. Thick lines show the FM/AFMD and AFMD/AFM1 phase boundaries. The cross corresponds to the global, symmetry-dictated [21,23] minimum (ground state). The path representing the simulation of the tensile test for loading along the [0 0 1] direction is denoted by full circles; the highest circle marked by an arrow corresponds to the maximum stress obtained in the simulation of the tensile test.

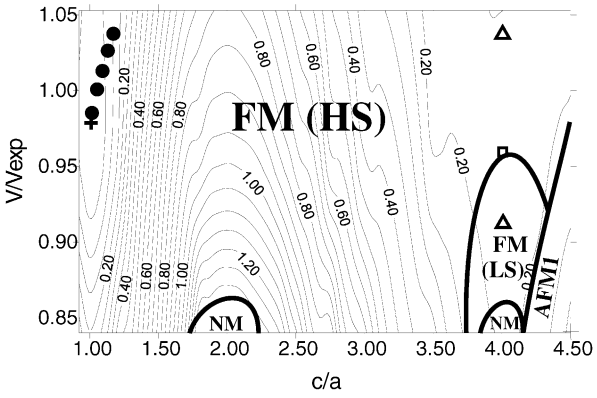

Fig. 2. Total energy (per atom) of iron as a function of the trigonal c/a ratio and volume relative to the energy of the FM bcc ground state, calculated within the GGA. Here the bcc structure corresponds to $c/a = 1$, the simple cubic structure to $c/a = 2$ and the fcc structure to $c/a = 4$ [23]. Only states with the minimum energy are shown. The contour interval is equal to 50 meV. Thick lines show the FM(HS)/NM, FM(HS)/FM(LS), FM(LS)/NM and FM(LS)/AFM1 phase boundaries. The cross corresponds to the global symmetry-dictated [21,23] minimum (ground state), the triangles show the local minima of the total energy of the fcc states in the FM(HS) and FM(LS) region at $V/V_{exp} = 1.037$ and 0.911, respectively. The square at $V/V_{exp} = 0.955$ denotes the crossing point of the dependences of the total energy of the FM(HS) and FM(LS) fcc states on volume. A more detailed analysis shows that this square represents a "sharp" saddle point [69]. The path representing simulation of the tensile test for loading along the [1 1 1] direction is denoted by full circles; the state corresponding to the maximum stress attained in the tensile test simulation ($V/V_{exp} = 1.114$, $c/a = 1.356$) lies outside the area of the figure.

and FM regions whereas the area of Fig. 2 is dominated by the FM states. The global minimum of energy is in the FM region at $c/a = 1$, $V/V_{\mathrm{exp}} = 0.985$, which corresponds to the bcc structure. The calculated equilibrium volume is about 1.5% lower than the experimental value, which we regard as a very good agreement.

Let us discuss the tetragonal case first (Fig. 1). Apart from the large FM area, there are AFMD and AFM1 regions in the neighborhood of the fcc structure, which corresponds to the line $c/a = \sqrt{2}$. In accordance with [89], we found that the fcc iron with the AFM1 or AFMD spin ordering is unstable with respect to the tetragonal deformation. A more detailed discussion of the tetragonal case is presented in [90,91]. In those papers, we also showed how the contour plot presented in Fig. 1 may be used to predict the lattice parameters and magnetic states of iron overlayers at (0 0 1) substrates.

The AFM1 and AFMD states with the trigonal symmetry have mostly higher energy than the FM states and, consequently, they are nearly invisible in Fig. 2, except for the lower right corner. However, two regions of the FM states may be found in Fig. 2: FM(HS), the high-spin states (with magnetic moment higher than about 2 μ_B) and FM(LS), the low-spin states (with magnetic moment lower than about 1.2 μ_B). There is a sharp discontinuity in the magnetic moment at the border FM(HS)/FM(LS). Nonetheless, the total energy remains surprisingly smooth. The triangles in Fig. 2 denote local energy minima of fcc FM states and the square marks the point where the volume dependences of the total energies of the fcc FM(HS) and FM(LS) states intersect.

4.1.2. Uniaxial and hydrostatic tensile tests

In accordance with the methodology described in Section 2, we performed the simulation of a tensile test in iron for uniaxial loading along the [0 0 1] and [1 1 1] directions as well as for loading by the negative hydrostatic pressure. The corresponding total energies as functions of the relative elongation ε are displayed in Fig. 3(a). In the case of the hydrostatic loading, ε corresponds to the relative extension of the bcc lattice parameter.

It is seen from Fig. 3(a) that the total energy profiles have a parabolic, convex character in the neighborhood of the ferromagnetic (FM) symmetry-dictated [21,23] minimum that corresponds to the bcc structure (ground state). With increasing ε the curves reach (due to non-linear effects) their inflexion points (marked by vertical lines in Fig. 3(a)) and become concave. The inflexion point for [0 0 1] uniaxial loading occurs (most likely incidentally) for nearly the same elongation of $\varepsilon = 0.15$ as for the hydrostatic loading. In the case of the [0 0 1] tensile test, this elongation corresponds to the lattice parameter in the direction of loading equal to 6.20 au (accompanied by relaxation in [1 0 0] and [0 1 0] directions in which the lattice constant decreases to 5.12 au) and, in the case of hydrostatic strain, to the bcc structure with the lattice constant of 6.20 au.

The tensile stresses calculated according to the formulas given in Section 2 are shown in Fig. 3(b). The inflexion points on the total energy profiles (Fig. 3(a)) correspond to maximum stresses (Fig. 3(b)) which the material may accommodate if its structure type does not change during the deformation. They are equal to $\sigma_{\mathrm{max}}^{[0\,0\,1]} = 12.7$ GPa (this value was reported in our previous work [67] and is not very different from the values of 14.2 and 12.6 GPa found in [68,71], respectively), $\sigma_{\mathrm{max}}^{[1\,1\,1]} = 27.3$ GPa [69,70] and $\sigma_{\mathrm{max}}^{[\mathrm{hydrostatic}]} = 27.9$ GPa [69,70] for uniaxial tensile test along the [0 0 1] and [1 1 1] direction and for hydrostatic loading, respectively. These values represent the theoretical tensile strengths provided other instabilities [14,31,38,42,69,71,73–78] do not come forth before the inflexion point has been reached. In the case of iron with its large variety of magnetic phases, another instability may originate from transitions between those phases. However, as it is seen from Figs. 1 and 2, no such transition appears during tensile tests along [0 0 1] and [1 1 1] directions (all states involved up to the maximum stress lie in the FM region). A similar situation arises for hydrostatic deformation [63]. Other conditions of stability [73–76] will be analyzed in a subsequent publication, but our preliminary calculations as well as the results presented in [71] for the [0 0 1] uniaxial deformation indicate that they will not be violated. It should be noted that the theoretical strength for loading in the [1 1 1] direction, equal to 27.3 GPa, is nearly the same as that obtained for hydrostatic loading, 27.9 GPa. At present, we do not have any plausible explanation of this fact.

In Fig. 3(a), it is seen that there are also maxima on the total energy versus ε dependence dictated by the symmetry [21,23]. They correspond to the fcc and simple cubic (sc) structures when simulating tensile tests with loading along the [0 0 1] and [1 1 1] directions, respectively. These maxima are denoted by arrows in Fig. 3(a). Their presence dictates that the corresponding dependence of the energy on elongation must level off, which imposes certain limitations on the maximum stress [27]. In the cases when there is no symmetry-dictated maximum (e.g. in the uniaxial tensile test along the [0 0 1] direction of NiAl with the B2 structure in the ground state [29]), the maximum stress is usually higher.

Since the structural energy difference $E_{\mathrm{sc}} - E_{\mathrm{bcc}}$ is about five times higher than the difference $E_{\mathrm{fcc}} - E_{\mathrm{bcc}}$ (755 meV/atom compared to 155 meV/atom), the E versus ε curve for the [1 1 1] loading must rise much higher, albeit for larger strains, than that for the [0 0 1] loading (see Fig. 3(a)). Consequently, for the tensile test in the [1 1 1] direction the inflexion point occurs at a higher strain and for a higher stress than in the test with loading in the [0 0 1] direction. Thus, similarly as for W [27], a marked anisotropy of ideal tensile strengths for the [0 0 1] and [1 1 1] loading directions may be understood in terms of the structural energy differences of nearby higher-symmetry structures found along the deformation path.

Relative changes of atomic volume and the dependences of the magnetic moment of FM iron are shown as functions of elongation in Fig. 3(c) and (d), respectively. In the neighborhood of the ground state structure the atomic vol-

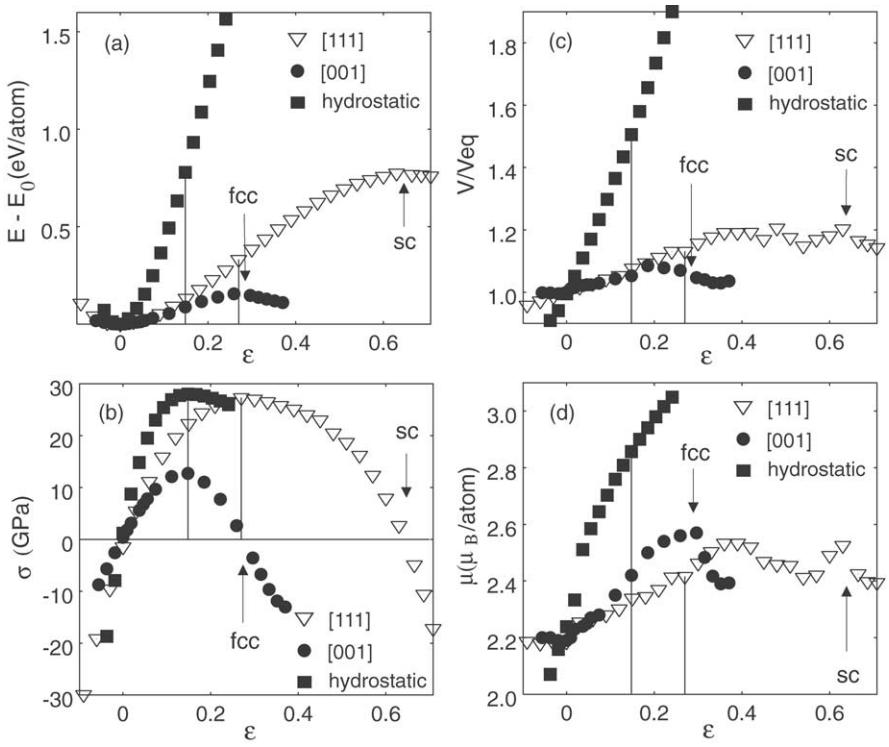

Fig. 3. Total energy (per atom) measured relative to the energy of the FM bcc ground state (a), tensile stress (b), relative atomic volume ratio measured relative to the equilibrium volume V_{eq} (c), and magnetic moment per atom μ (d) of FM iron loaded hydrostatically (full squares) and uniaxially along the [0 0 1] (full circles) and [1 1 1] (empty triangles) directions versus the elongation ε. The relative elongation ε reflects the changes of the lattice parameter a_{bcc} for hydrostatic loading and, in the case of uniaxial tensile tests, the increase/decrease of the crystal dimension in the directions of loading. The thin vertical lines mark the states exhibiting maximum stress (i.e. theoretical tensile strength), sc means the simple cubic structure. Incidentally, the maximum stresses for [0 0 1] uniaxial and hydrostatic loading are reached at nearly the same strain ε.

ume increases with increasing elongation but it exhibits a more complex behaviour at larger deformations. For hydrostatic loading, the magnetic moment shows monotonous increase with increasing volume (in agreement with Herper et al. [92]) while in tensile tests it exhibits local extrema at points corresponding to higher-symmetry structures (maxima for fcc and simple cubic) as well as at some other points along the paths.

4.2. Intermetallic compound Ni_3Al

In contrast with iron, in the case of Ni_3Al we start with the fcc-based $L1_2$ structure. For this purpose, we renormalize the ratio c/a by ascribing the value of $c/a = 1$ to the $L1_2$ structure. As a result, the c/a for the tetragonal path is by a factor of $\sqrt{2}$ smaller and for the trigonal path by a factor of 4 smaller than in the case of iron.

Using the GGA, the minimum of the total energy is obtained for the ferromagnetic state with the lattice constant equal to 3.561 Å (6.729 au) and magnetic moment of 0.80 μ_B per formula unit. The lattice constant agrees very well with the experimental value [93] of 3.568 Å (6.743 au) whereas the experimental magnetic moment, 0.23 μ_B per formula unit, is much lower. When including the spin-orbit coupling, Xu et al. [94] obtained 0.46 μ_B per formula unit, which is closer to the experimental value. At present, we are verifying this conclusion.

There is a very small energy difference between the FM and NM state of the $L1_2$ structure—only 21.3 meV/formula unit. This is consistent with the results of Xu et al. [94] (0.2–0.5 mRy/f.u.) and Min et al. [95] (∼1 mRy/f.u.).

Fig. 4 displays the total energy of Ni_3Al as a function of the volume and c/a for the trigonal deformation. Again, we show only those states the energies of which are the lowest for a given configuration. A nearly vertical border divides the area of Fig. 4 into FM and NM regions. There is a saddle point for $c/a = 0.5$ and $V/V_{exp} \sim 1.2$ (outside the area of the figure). The minimum at $c/a \approx 0.27$, $V/V_{exp} \approx 1.01$ is not dictated by symmetry.

Fig. 5 shows the total energy of Ni_3Al as a function of the volume and c/a for the tetragonal deformation. Here NM regions extend to both sides of the FM ground state. However, there are no energy extrema and saddle points in those NM regions. It is interesting that the transition from the FM to NM state during both the trigonal and tetragonal deformation is essentially continuous, with no discontinuities in magnetic moment. Xu et al. [94] have shown that the energy gain in Ni_3Al associated with magnetism is about an order of magnitude smaller than that due to the structural differences. Our calculations show that the NM Ni_3Al in the $L1_2$

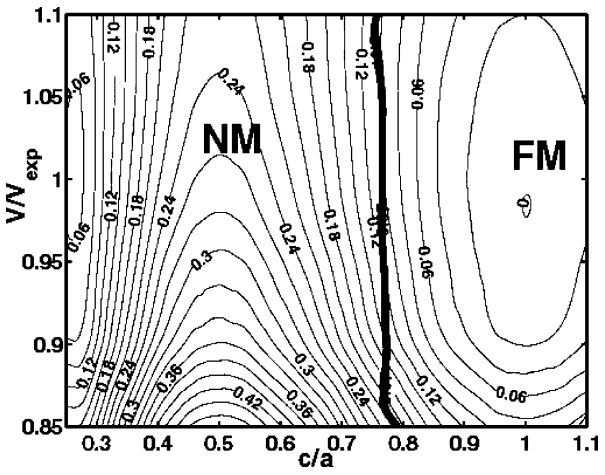

Fig. 4. Total energy (per formula unit) of Ni_3Al as a function of the volume and c/a ratio, characterizing the trigonal deformation, calculated within the GGA. The energy is measured relative to the energy of the FM $L1_2$ ground state (the minimum at $c/a = 1$). Only states with the minimum energy are shown. The contour interval is 20 mRy. Thick line shows the NM/FM phase boundary. The ground-state minimum at $c/a = 1$ and the saddle point at $c/a = 0.5$ (outside the figure area) are dictated by symmetry.

structure is stable with respect to tetragonal and trigonal deformations (the shear moduli $C' = (C_{11} - C_{12})/2$ and C_{44} are nearly the same for the NM and FM states). Therefore, magnetism does not appear to play any important role in the control of phase stability. This is in sharp contrast with iron, where the onset of ferromagnetism stabilizes the bcc structure and NM bcc states are not stable with respect to the tetragonal deformation [90,91].

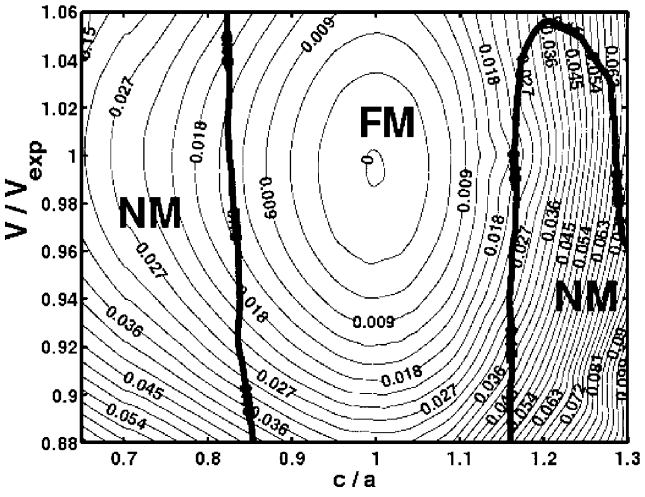

Fig. 5. Total energy (per formula unit) of Ni_3Al as a function of the volume and c/a ratio, characterizing the tetragonal deformation, calculated within the GGA. The energy is measured relative to the energy of the FM $L1_2$ ground state (the minimum at $c/a = 1$). Only states with the minimum energy are shown. The contour interval is 3 mRy. Thick lines show the NM/FM phase boundaries. The only symmetry-dictated extremum is at $c/a = 1$.

Table 1
Theoretical tensile strengths σ_{th} calculated ab initio

Material	Structure	Direction	σ_{th} (GPa)	Reference
Fe	A2	[1 1 1]	27.3	[69,70]
		[0 0 1]	12.7	[67,69,70]
		[0 0 1]	14.2	[68]
		[0 0 1]	12.6	[71]
W	A2	[0 0 1]	28.9	[27]
		[0 0 1]	29.5	[37]
		[1 1 1]	40.1	[27]
		[1 1 0]	54.3	[27]
Al	A1	[0 0 1]	12.1[a]	[31]
		[0 0 1]	13.1[b]	[54]
		[0 0 1]	9.20[c]	[78]
		[1 1 1]	11.05	[31]
		[1 1 1]	11[b]	[32,33]
		[1 1 1]	8.95[c]	[78]
		[1 1 0]	4.89[c]	[78]
Cu	A1	[0 0 1]	55[b], 32[b]	[17]
		[0 0 1]	33	[30]
		[0 0 1]	9.4[a]	[77]
		[1 1 0]	31	[30]
		[1 1 1]	29	[30]
diamond	A4	[1 1 1]	90	[40]
		[1 1 1]	95	[41]
		[0 0 1]	225	[40]
		[0 0 1]	130	[40]
Si	A4	[0 0 1]	22	[41]
Ge	A4	[0 0 1]	14	[41]
Nb	A2	[0 0 1]	13.1[a]	[42]
Mo	A2	[0 0 1]	28.8	[42]
TiC	B1	[0 0 1]	44	[26]
NiAl	B2	[0 0 1]	46	[29,30]
		[1 1 1]	25	[29,30]
β-SiC	B3 (3C)	[0 0 1]	101	[39]
		[1 1 1]	50.8	[39]
AlN	B4	[0 0 0 1]	50[b]	[32,33]
$MoSi_2$	$C11_b$	[0 0 1]	37	[64–66]
WSi_2	$C11_b$	[0 0 1]	38	[64–66]
β-Si_3N_4	$P6_3/m$	[1 0 0]	72.2[b]	[43]
		[1 0 0]	57	[45]
		[0 0 1]	75.0[b]	[43]
		[0 0 1]	55	[45]
c-Si_3N_4	$Fd\bar{3}m$	[0 0 1]	45	[44]
Ni_3Al	$L1_2$	[0 0 1]	17.5	Present work
		[1 1 1]	33.7	Present work

[a] The values which correspond to violation of some another elastic stability criterion prior to reaching the inflexion point at the energy vs. elongation dependence.

[b] The perpendicular dimensions of the sample were not relaxed during the calculations (no Poisson contraction allowed).

[c] The values obtained from the phonon instabilities.

Now, we can also simulate tensile tests in Ni_3Al in order to get theoretical tensile strengths for uniaxial loading along the [0 0 1] and [1 1 1] directions. For the [0 0 1] loading, the maximum stress corresponding to the inflexion point on the total energy versus ε curve is $\sigma_{max}^{[0\,0\,1]} = 17.5\,GPa$, and for the [1 1 1] loading $\sigma_{max}^{[1\,1\,1]} = 33.7\,GPa$.

5. Ab initio calculated values of theoretical tensile strength

For the sake of completeness, we summarize in Table 1 all ab initio calculated values of the theoretical tensile strength (including relaxation in directions perpendicular to the loading axis and, if applicable, of internal structure parameters) that have been evaluated until now. Most of them correspond to the inflexion point on the strain dependence of the total energy. Non-relaxed calculations are also included; the corresponding values are denoted by "*b*". As for the strength of W for [1 1 0] loading, the material probably breaks down due to some other instability before reaching the inflexion point and, therefore, the true theoretical tensile strength will be lower than that given in the table. The situation is most likely the same in the case of Cu where the experimental ideal strengths are about an order of magnitude lower than the calculated ones [30]. Semiempirical calculations [96] indeed suggest that, for the [0 0 1] direction, the tetragonal shear modulus C' becomes zero (i.e., the tetragonal structure is not stable with respect to transformation to an orthorombic structure) well before reaching the inflexion point. It may be expected that similar instabilities will occur for the [1 1 0] and [1 1 1] orientations. Our recent ab initio investigation [77] yields $\sigma_{max}^{[0\,0\,1]} = 9.4\,GPa$ for $C' = 0$, still substantially higher than the experimental result of 1.5 GPa. Possible reasons of this disagreement are discussed in [77].

6. What is the role of ab initio electronic structure calculations in contemporary studies of the strength of materials?

The significance of ab initio (first-principles) electronic structure calculations is in high reliability predicting new properties and phenomena. There are no adjustable parameters and well-defined approximations are introduced on the most fundamental level. Many basic material properties may be calculated and extensive databases may be generated. However, we should emphasize here that the goal of the ab initio electronic structure calculations is not merely to obtain numbers, but rather insights. The results include, for example, electronic wavefunctions, charge densities, bond characteristics etc. By variation of some parameters of the calculations we can learn which aspect of a given problem is important. Analyzing total energy as a function of deformation and corresponding stability conditions, strength of defect-free bulk material as well as of nanowires, grain boundaries and other interfaces may be safely determined.

The state-of-the-art ab initio calculations are computationally very intensive and only relatively small number of non-equivalent atoms (up to several hundreds) may be relaxed. For more complicated cases, e.g. for atomistic studies of mechanical properties of real materials containing dislocations, we have to resort to simpler methods using semiempirical interatomic potentials with adjustable parameters, such as Finnis–Sinclair potentials, embedded atom method, bond-order potentials, or model generalized pseudopotential theory [97–100]. To get reliable interatomic potentials, one should include into the fitting procedure also some high-energy configurations the properties of which can be calculated by ab initio methods. This will enhance the accuracy and transferability of such potentials considerably since other regions of the "configurational space" that are not accessible experimentally are taken into account. These "less fundamental" approaches, employed in very extensive atomic-level studies including simulation of defect structures and their strength, proved to be extremely useful in investigating generic phenomena in many systems, but they often do not provide the desired physical accuracy for a specific material.

Extensive testing of these "less fundamental" methods must always be carried out. Here again ab initio calculations may be used for benchmarking of these approaches checking, for example, their results for simple configurations not used in the potential construction and showing us the limits of their reliability and accuracy.

Ab initio electronic structure calculations are indispensable when a phenomenon studied is controlled directly by the electronic structure and cannot be captured by common interatomic potentials. Behaviour of magnetic materials under large deformation studied in this paper or magnetism of grain boundaries constitute such examples.

The calculated values of the theoretical strength and other quantities may serve as input parameters to quantitative models employing standard dislocation theory, that describes the relationship between the yield behaviour and length-scale effects in the nanoscale regime. Such models will complement and enhance the strain gradient models of continuum mechanics dealing with deformation of materials subject to inhomogeneous loads on nano- and microscale. This combined approach will contribute to a deeper understanding of the onset of yielding in nanoindentation and of some other aspects of deformation in materials subject to large inhomogeneous loads.

In general, to attain the full understanding of phenomena studied, it is often imperative to combine simpler methods with ab initio calculations on one side and experiment on the other. This approach is more and more applied in multiscale modeling of materials [101–103]. One of the main goals of such activities is to develop predictive methods and algorithms to understand properties of materials, including their strength, plastic behaviour and fracture.

Acknowledgements

This research was supported by the Grant Agency of the Academy of Sciences of the Czech Republic (Project No. IAA1041302), by the Grant Agency of the Czech Republic (Project No. 202/03/1351), by the Research Project Z2041904 of the Academy of Sciences of the Czech Republic, and by the U.S. Department of Energy, Basic Energy Sciences (Grant No. DE-FG02-98ER45702). A part of this study has been performed in the framework of the COST Project No. OC 523.90. The use of the computer facilities at the MetaCenter of the Masaryk University, Brno, and at the Boston University Scientific Computing and Visualization Center is acknowledged.

References

[1] P. Hohenberg, W. Kohn, Phys. Rev. 136 (1964) B864.
[2] W. Kohn, L.J. Sham, Phys. Rev. 140 (1965) A1133.
[3] R.G. Parr, W. Yang, Density-functional Theory for Atoms and Molecules, Oxford University Press, Oxford, New York, 1989.
[4] S.S. Brenner, J. Appl. Phys. 27 (1956) 1484.
[5] S.S. Brenner, J. Appl. Phys. 28 (1957) 1023.
[6] R.V. Coleman, B. Price, N. Cabrera, J. Appl. Phys. 28 (1957) 1360.
[7] G.L. Pearson, W.T. Read Jr., W.L. Feldmann, Acta Met. 5 (1957) 181.
[8] E.M. Nadgornyi, Usp. Fiz. Nauk 77 (1962) 201 [English Trans.: Sov. Phys. Uspekhi 5 (1962) 462].
[9] R.P. Vinci, J.J. Vlassak, Ann. Rev. Mater. Sci. 26 (1996) 431.
[10] D.F. Bahr, D.E. Kramer, W.W. Gerberich, Acta Mater. 46 (1998) 3605.
[11] A. Gouldstone, H.J. Koh, K.Y. Zeng, A.E. Giannakopoulos, S. Suresh, Acta Mater. 48 (2000) 2277.
[12] C.L. Woodcock, D.F. Bahr, Scripta Mater. 43 (2000) 783.
[13] O.R. delaFuente, J.A. Zimmerman, M.A. Gonzalez, J. delaFiguera, J.C. Hamilton, W.W. Pai, J.M. Rojo, Phys. Rev. Lett. 88 (2002) 036101.
[14] K.J. van Vliet, J. Li, T. Zhu, S. Yip, S. Suresh, Phys. Rev. B 67 (2003) 104105.
[15] F. Milstein, S. Chantasiriwan, Phys. Rev. B 58 (1998) 6006.
[16] P. Šandera, J. Pokluda, Scripta Metall. Mater. 29 (1993) 1445.
[17] E. Esposito, A.E. Carlsson, D.D. Ling, H. Ehrenreich, C.D. Gelatt Jr., Phil. Mag. 41 (1980) 251.
[18] A.T. Paxton, P. Gumbsch, M. Methfessel, Phil. Mag. Lett. 63 (1991) 267.
[19] W. Xu, J.A. Moriarty, Phys. Rev. B 54 (1996) 6941.
[20] P. Söderlind, J.A. Moriarty, Phys. Rev. B 57 (1998) 10340.
[21] P.J. Craievich, M. Weinert, J.M. Sanchez, R.E. Watson, Phys. Rev. Lett. 72 (1994) 3076.
[22] L. Vitos, J. Kollár, H.L. Skriver, in: A. Gonis, P.E.A. Turchi, J. Kudrnovský (Eds.), Stability of Materials, Plenum Press, New York, London, 1996, p. 393.
[23] M. Šob, L.G. Wang, V. Vitek, Comp. Mat. Sci. 8 (1997) 100.
[24] P.J. Craievich, J.M. Sanchez, R.E. Watson, M. Weinert, Phys. Rev. B 55 (1997) 787.
[25] P. Alippi, P.M. Marcus, M. Scheffler, Phys. Rev. Lett. 78 (1997) 3892.
[26] D.L. Price, B.R. Cooper, J.M. Wills, Phys. Rev. B 46 (1992) 11368.
[27] M. Šob, L.G. Wang, V. Vitek, Mater. Sci. Eng. A 234–236 (1997) 1075.
[28] I.M. Mikhailovskii, I.Ya. Poltinin, L.I. Fedorova, Fizika Tverdogo Tela 23 (1981) 1291 [English Trans.: Sov. Phys. Solid State 23 (1981) 757].
[29] M. Šob, L.G. Wang, V. Vitek, Phil. Mag. B 78 (1998) 653.
[30] M. Šob, L.G. Wang, V. Vitek, Kovové materiály (Metall. Mater.) 36 (1998) 145.
[31] W. Li, T. Wang, J. Phys.: Condens. Matter 10 (1998) 9889.
[32] H. Kitagawa, S. Ogata, Key Eng. Mater. 161–163 (1999) 443.
[33] S. Ogata, H. Kitagawa, Comp. Mat. Sci. 15 (1999) 435.
[34] D. Roundy, C.R. Krenn, M.L. Cohen, J.W. Morris Jr., Phys. Rev. Lett. 82 (1999) 2713.
[35] D. Roundy, C.R. Krenn, J.W. Morris Jr., M.L. Cohen, Mater. Sci. Eng. A 317 (2001) 44.
[36] D. Roundy, C.R. Krenn, J.W. Morris Jr., M.L. Cohen, Mater. Sci. Eng. A 319–321 (2001) 111.
[37] D. Roundy, C.R. Krenn, M.L. Cohen, J.W. Morris Jr., Phil. Mag. A 81 (2001) 1725.
[38] J.W. Morris Jr., C.R. Krenn, Phil. Mag. A 80 (2000) 2827.
[39] W. Li, T. Wang, Phys. Rev. B 59 (1999) 3993.
[40] R.H. Telling, C.J. Pickard, M.C. Payne, J.E. Field, Phys. Rev. Lett. 84 (2000) 5160.
[41] D. Roundy, M.L. Cohen, Phys. Rev. B 64 (2001) 212103.
[42] W. Luo, D. Roundy, M.L. Cohen, J.W. Morris Jr., Phys. Rev. B 66 (2002) 094110.
[43] S. Ogata, N. Hirosaki, C. Kocer, H. Kitagawa, Phys. Rev. B 64 (2001) 172102.
[44] C. Kocer, N. Hirosaki, S. Ogata, Phys. Rev. B 67 (2003) 035210.
[45] S. Ogata, N. Hirosaki, C. Kocer, Y. Shibutani, J. Mater. Res. 18 (2003) 1168.
[46] S.-H. Jhi, S.G. Louie, M.L. Cohen, J.W. Morris Jr., Phys. Rev. Lett. 87 (2001) 075503.
[47] Y. Umeno, T. Kitamura, Mater. Sci. Eng. B 88 (2002) 79.
[48] S. Ogata, J. Li, S. Yip, Science 298 (2002) 807.
[49] G. Galli, F. Gygi, A. Catellani, Phys. Rev. Lett. 82 (1999) 3476.
[50] F.J. Ribeiro, D.J. Roundy, M.L. Cohen, Phys. Rev. B 65 (2002) 153401.
[51] M. Kohyama, Mater. Sci. Forum 294–296 (1999) 657.
[52] J.C. Hamilton, M. Foiles, Phys. Rev. B 65 (2002) 064104.
[53] M. Kohyama, Phys. Rev. B 65 (2002) 184107.
[54] T. Kitamura, Y. Umeno, Modell. Simul. Mater. Sci. Eng. 11 (2003) 127.
[55] I.G. Batirev, A. Alavi, M.W. Finnis, T. Deutsch, Phys. Rev. Lett. 82 (1999) 1510.
[56] S. Tanaka, R. Yang, M. Kohyama, in: Proceedings of the IUTAM Symposium on Mesoscopic Dynamics of Fracture Process and Materials Strength, Osaka, Japan, July 6–11, 2003, Solid Mechanics and its Applications, Kluwer Academic Publishers, Dordrecht, The Netherlands; Proceedings of the International Symposium on Micro-Mechanical Engineering—Heat Transfer, Fluid Dynamics, Reliability and Mechanotronics, ISMME2003, Tsuchiura, Tsukuba, Japan, December 1–3, 2003, The Japan Society of Mechanical Engineers, Tokyo 2003, paper B26-053.
[57] P. Šandera, J. Pokluda, L.G. Wang, M. Šob, Mater. Sci. Eng. A 234–236 (1997) 370.
[58] Y. Song, R. Yang, D. Li, W.T. Wu, Z.X. Guo, Phys. Rev. B 59 (1999) 14220.
[59] M. Černý, P. Šandera, J. Pokluda, Czech. J. Phys. 49 (1999) 1495.
[60] Y. Song, R. Yang, D. Li, Z.X. Guo, Phil. Mag. A 81 (2001) 321.
[61] Y. Song, Z.X. Guo, R. Yang, Phil. Mag. A 82 (2002) 1345.
[62] Y. Song, R. Yang, Z.X. Guo, Mater. Trans. 43 (2002) 3028.
[63] M. Černý, J. Pokluda, P. Šandera, M. Friák, M. Šob, Phys. Rev. B 67 (2003) 035116.
[64] M. Friák, M. Šob, V. Vitek, in: J.H. Schneibel, K.J. Hemker, R.D. Noebe, S. Hanada, G. Sauthoff (Eds.), High-temperature Ordered Intermetallic Alloys IX, Materials Research Society Symposium Proceedings, vol. 646, Materials Research Society, Warrendale, PA, 2001, paper N4.8.

[65] M. Friák, M. Šob, V. Vitek, Phys. Rev. B 68 (2003) 184101.
[66] M. Šob, M. Friák, V. Vitek, in: Proceedings of the International Symposium on Micro-mechanical Engineering—Heat Transfer, Fluid Dynamics, Reliability and Mechanotronics, ISMME2003, Tsuchiura, Tsukuba, Japan, December 1–3, 2003, The Japan Society of Mechanical Engineers, Tokyo, 2003, paper B26-051.
[67] M. Friák, M. Šob, V. Vitek, in: Proceedings of the International Conference Juniormat'01, Institute of Materials Engineering, Brno University of Technology, Brno, 2001, pp. 117–120.
[68] D.M. Clatterbuck, D.C. Chrzan, J.W. Morris Jr., Phil. Mag. Lett. 82 (2002) 141.
[69] M. Šob, M. Friák, D. Legut, V. Vitek, in: P.E.A. Turchi, A. Gonis (Eds.), Proceedings of the Third International Alloy Conference: An Interdisciplinary Approach to the Science of Alloys in Metals, Minerals and Other Materials Systems, Estoril/Cascais, Portugal, June 30–July 5, 2002, in press.
[70] M. Friák, M. Šob, V. Vitek, Phil. Mag. 83 (2003) 3529.
[71] D.M. Clatterbuck, D.C. Chrzan, J.W. Morris Jr., Acta Mater. 51 (2003) 2271.
[72] D.M. Clatterbuck, D.C. Chrzan, J.W. Morris Jr., Scripta Mater. 49 (2003) 1007.
[73] R. Hill, F. Milstein, Phys. Rev. B 15 (1977) 3087.
[74] J. Wang, J. Li, S. Yip, S. Phillpot, D. Wolf, Phys. Rev. B 52 (1995) 12627.
[75] Z. Zhou, B. Joós, Phys. Rev. B 54 (1996) 3841.
[76] K.Y. Kim, Phys. Rev. B 54 (1996) 6245.
[77] M. Černý, M. Šob, J. Pokluda, P. Šandera, J. Phys.: Condens. Matter 16 (2004) 1045.
[78] D.M. Clatterbuck, C.R. Krenn, M.L. Cohen, J.W. Morris Jr., Phys. Rev. Lett. 91 (2003) 135501.
[79] M. Šob, L.G. Wang, M. Friák, V. Vitek, in: M. Cross, J.W. Evans, C. Bailey (Eds.), Computational Modeling of Materials, Minerals, and Metals Processing, The Minerals, Metals and Materials Society, Warrendale, PA, 2001, pp. 715–724.
[80] J.W. Morris Jr., C.R. Krenn, D. Roundy, M.L. Cohen, in: P.E.A. Turchi, A. Gonis (Eds.), Phase Transformations and Evolution in Materials, The Minerals, Metals and Materials Society, Warrendale, PA, 2000, pp. 187–207.
[81] J. Pokluda, P. Šandera, in: T. Prnka, (Eds.), Proceedings of the Ninth International Metallurgical Conference METAL 2000, Tanger, Ostrava, Czech Republic, May 16–18, 2000.
[82] J. Pokluda, P. Šandera, M. Černý, M. Šob, in preparation.
[83] D.J. Singh, Planewaves, Pseudopotentials and the LAPW Method, Kluwer Academic Publishers, Boston, 1994.
[84] I. Turek, V. Drchal, J. Kudrnovský, M. Šob, P. Weinberger, Electronic Structure of Disordered Alloys, Surfaces and Interfaces, Kluwer Academic Publishers, Boston, 1997.
[85] V.V. Nemoshkalenko, V.N. Antonov, Computational Methods in Solid State Physics, Gordon and Breach Science Publishers, Amsterdam, 1998.
[86] M. Springborg, Methods of Electronic-structure Calculations, Wiley, Chichester, 2000.
[87] P. Blaha, K. Schwarz, J. Luitz, WIEN97, Technical University of Vienna 1997—improved and updated Unix version of the original copyrighted WIEN-code, which was published by P. Blaha, K. Schwarz, P. Sorantin, S.B. Trickey, Comput. Phys. Commun. 59 (1990) 399.
[88] J.P. Perdew, S. Burke, M. Ernzerhof, Phys. Rev. Lett. 77 (1996) 3865.
[89] S.L. Qiu, P.M. Marcus, H. Ma, J. Appl. Phys. 87 (2000) 5932.
[90] M. Friák, M. Šob, V. Vitek, Phys. Rev. B 63 (2001) 052405.
[91] M. Friák, M. Šob, V. Vitek, in: A. Gonis, N. Kioussis, M. Ciftan (Eds.), Electron Correlations and Material Properties 2, Kluwer Academic Publishers, Boston, 2003, pp. 399–415.
[92] H.C. Herper, E. Hoffmann, P. Entel, Phys. Rev. B 60 (1999) 3839.
[93] F.R. de Boer, C.J. Schinkel, J. Biesterbos, S. Proost, J. Appl. Phys. 40 (1969) 1049.
[94] J. Xu, B.I. Min, A.J. Freeman, T. Oguchi, Phys. Rev. B 41 (1990) 5010.
[95] B.I. Min, A.J. Freeman, H.J.F. Jansen, Phys. Rev. B 37 (1988) 6757.
[96] F. Milstein, B. Farber, Phys. Rev. Lett. 44 (1980) 277.
[97] V. Vitek, Mater. Res. Soc. Bull. 21 (2) (1996) 17.
[98] D.G. Pettifor, I.I. Oleinik, D. Nguyen-Manh, V. Vitek, Comp. Mat. Sci. 23 (2002) 33.
[99] M. Mrověc, V. Vitek, D. Nguyen-Manh, D.G. Pettifor, L.G. Wang, M. Šob, in: D.H. Lassila, I.M. Robertson, R. Phillips, B. Devincre (Eds.), Multiscale Phenomena in Materials—Experiment and Modeling, MRS Symposium Proceedings, vol. 578, Materials Research Society, Warrendale, PA, 2000, pp. 199–204.
[100] J.A. Moriarty, J.F. Belak, R.E. Rudd, P. Söderlind, F.H. Streitz, L.H. Yang, J. Phys.: Condens. Matter 14 (2002) 2825.
[101] Multiscale Modeling of Materials 2000, in: L. Kubin, R.L. Selinger, J.L. Bassani, K. Cho (Eds.), Material Research Society Symposium Proceedings, vol. 653, Materials Research Society, Warrendale, PA, 2001.
[102] R. Phillips, Crystals, Defects and Microstructures: Modeling Across Scales, Cambridge University Press, Cambridge, 2001.
[103] R.M. Nieminen, J. Phys. Cond. Matter 14 (2002) 2859.